nature structural & molecular biology

Structural basis for plasmepsin V inhibition that blocks export of malaria proteins to human erythrocytes

Anthony N Hodder[1,2,4], Brad E Sleebs[1,2,4], Peter E Czabotar[1,2,4], Michelle Gazdik[1,2], Yibin Xu[1], Matthew T O'Neill[1], Sash Lopaticki[1], Thomas Nebl[1], Tony Triglia[1], Brian J Smith[3], Kym Lowes[1], Justin A Boddey[1,2] & Alan F Cowman[1,2]

Plasmepsin V, an essential aspartyl protease of malaria parasites, has a key role in the export of effector proteins to parasite-infected erythrocytes. Consequently, it is an important drug target for the two most virulent malaria parasites of humans, *Plasmodium falciparum* and *Plasmodium vivax*. We developed a potent inhibitor of plasmepsin V, called WEHI-842, which directly mimics the *Plasmodium* export element (PEXEL). WEHI-842 inhibits recombinant plasmepsin V with a half-maximal inhibitory concentration of 0.2 nM, efficiently blocks protein export and inhibits parasite growth. We obtained the structure of *P. vivax* plasmepsin V in complex with WEHI-842 to 2.4-Å resolution, which provides an explanation for the strict requirements for substrate and inhibitor binding. The structure characterizes both a plant-like fold and a malaria-specific helix-turn-helix motif that are likely to be important in cleavage of effector substrates for export.

Plasmepsin V is an aspartic acid protease expressed by protozoan parasites of *Plasmodium* species, and it has a crucial role in recognizing and processing effector proteins for export to host cells[1,2]. *P. falciparum* and *P. vivax*, which are responsible for the most severe forms of malaria, infect humans through bites by infected *Anopheles* mosquitos. The parasites then migrate to the liver and develop into merozoites, which are released, invade the erythrocytes in which they develop and then amplify through successive rounds of infection. Effector proteins exported to the host cell by these parasites[3,4] are responsible for a remarkable process of cellular renovation that is induced in parasite-infected erythrocytes[5]. Remodeling of the host cell provides a means for the parasite to gain nutrients and remain hidden from the host's responses in a relatively protected niche.

Plasmepsin V is a type I integral membrane-bound protease with the active domain located on the luminal side of the endoplasmic reticulum (ER)[1,2,6]. It recognizes and cleaves a pentameric sequence (RxLxE-Q-D) known as the PEXEL[3], or vacuolar transport signal[4] on the carboxy side of the leucine residue[7,8]; when this motif is located 15–30 amino acids C terminal to a hydrophobic ER-type signal sequence, proteins are exported[3,4,9]. This processing step by plasmepsin V uncovers the export signal (xE-Q-D) and directs these proteins to the plasma membrane and the parasitophorous vacuole membrane[1,2,6,8] that surrounds the parasite, where they are recognized by the *Plasmodium* translocon of exported proteins, a protein machine that translocates them into parasite-infected erythrocytes[10,11].

Cleavage of the PEXEL motif by plasmepsin V is essential for protein export in *P. falciparum*–infected erythrocytes because the gene encoding this enzyme cannot be disrupted[1,12]. In addition, expression of a dominant-negative form of plasmepsin V in *P. falciparum* results in reduced export of proteins to the host erythrocyte and impaired growth, thus suggesting that plasmepsin V is indeed required for this trafficking pathway[2,6]. A PEXEL-mimetic compound containing statine, a molecule with a hydroxyl functionality that mimics the transition state of amide-bond proteolysis, inhibits *in vitro* activity of *P. falciparum* and *P. vivax* plasmepsin V, blocks protein export and lethally inhibits *P. falciparum* growth[6]. This inhibition by a PEXEL-mimicking small molecule has shown that plasmepsin V plays a crucial part in protein export and that this process is essential for parasite survival, thus validating this enzyme as an important antimalarial target in asexual blood stages. Currently, to our knowledge there are no three-dimensional structures of plasmepsin V. However, a structure would probably accelerate the development of more drug-like inhibitors of this drug target.

To understand the structure of plasmepsin V, we developed a new and potent inhibitor that allowed us to solve the first crystallographic structure, which included the inhibitor compound bound *in situ* to the active site of the enzyme. This structure has provided an unprecedented level of detail that explains how substrates and inhibitors dock in the active site and indicates two unique domains that are probably important for the function of plasmepsin V during the export process.

RESULTS

A potent inhibitor of plasmepsin V

The most potent inhibitor to date, WEHI-916 (**Fig. 1a**), has a high affinity for the endogenous enzyme but has a modest ability to inhibit *P. falciparum* growth[6,13]. We postulated the latter was due to the highly

[1]Walter and Eliza Hall Institute of Medical Research, Parkville, Victoria, Australia. [2]Department of Medical Biology, University of Melbourne, Parkville, Victoria, Australia. [3]La Trobe Institute for Molecular Science, La Trobe University, Victoria, Australia. [4]These authors contributed equally to this work. Correspondence should be addressed to A.F.C. (cowman@wehi.edu.au) or J.A.B. (boddey@wehi.edu.au).

Received 7 May; accepted 29 June; published online 27 July 2015; doi:10.1038/nsmb.3061

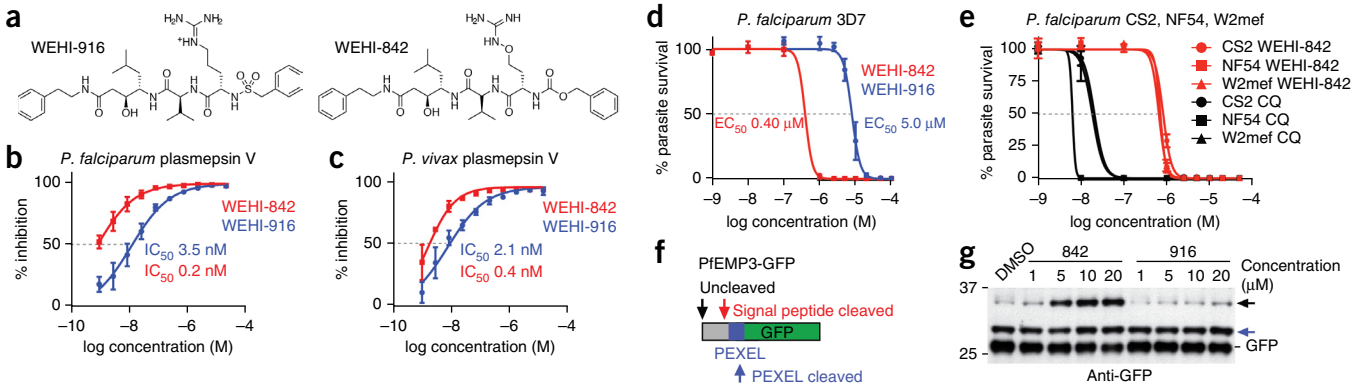

Figure 1 Structures of WEHI-842 and WEHI-916 and effect on plasmepsin V function. (**a**) Structures of the transition-state mimetics WEHI-916 and WEHI-842, corresponding to the RVL PEXEL. (**b**,**c**) Effects of WEHI-842 and WEHI-916 on plasmepsin V activity. Inhibition of *P. falciparum* (*Pf*) (**b**) and *P. vivax* (*Pv*) (**c**) plasmepsin V with KAHRP fluorogenic substrate. Data points represent means ± s.d. for three independent experiments. IC_{50}, half-maximal inhibitory concentration. (**d**) Growth inhibition of *P. falciparum* strain 3D7 (chloroquine sensitive) by WEHI-842 and WEHI-916. EC_{50}, half-maximal effective concentration. Data represent mean ± s.e.m. for three independent experiments. (**e**) Growth inhibition of *P. falciparum* strains CS2, W2mef (chloroquine resistant) and NF54 (chloroquine sensitive) by WEHI-842 and chloroquine (CQ). Data represent mean ± s.e.m. for three independent experiments. (**f**) Structure of the exported PfEMP3-GFP chimeric protein expressed in *P. falciparum*. (**g**) Effects of WEHI-842 and WEHI-916 (3 h) on cleavage of the PEXEL in PfEMP3-GFP. Black arrow, uncleaved protein accumulating in the ER from inhibition of plasmepsin V; blue arrow, plasmepsin V–cleaved band. Bottom, anti-HSP70 loading control. (**h**) Effects of WEHI-842 and WEHI-916 (10 µM) on cleavage of PEXEL in PfEMP3-GFP. Bottom, anti-HSP70 loading control. Data shown in **g** and **h** are representative of two independent experiments. Uncropped images are shown in **Supplementary Data Set 1**.

polarized guanidinium group on the P_3 arginine of WEHI-916. Guanidinium groups are known to impede the membrane permeability of small molecules, and this can be overcome by replacement with a guanidine isostere[14,15]. Because the guanidinium group on the P_3 arginine is essential for binding affinity[6,13,16], we selected the nonproteinogenic amino acid canavanine to replace the P_3 arginine, thus conserving the interactions with plasmepsin V. The new compound, WEHI-842 (**Fig. 1a**), also has an N-terminal carbamate replacing the sulfonamide in WEHI-916, a modification known not to affect the binding affinity to plasmepsin V[13].

We produced recombinant *P. falciparum* and *P. vivax* plasmepsin V (**Supplementary Fig. 1a**,**b**) and tested the effects of WEHI-842 and WEHI-916 on enzyme activity. The plasmepsin V proteins demonstrated a specific activity against PEXEL substrates (**Supplementary Fig. 1c**–**e**), with kinetics similar to previous measurements for endogenous proteins[6]. The K_m for recombinant plasmepsin V with a fluorogenic PEXEL substrate from the knob-associated histidine-rich protein (KAHRP) was 20.2 ± 3.7 µM (mean ± s.d.) and 6.0 ± 0.3 µM for the *P. falciparum* and *P. vivax* enzymes, respectively (**Supplementary Fig. 1f**–**l**).

WEHI-842, compared to WEHI-916, had a substantially increased potency against recombinant *P. falciparum* plasmepsin V (**Fig. 1b**). We also observed a similar difference in potency between the two compounds against *P. vivax* plasmepsin V (**Fig. 1c**). Binding affinities of WEHI-842 and WEHI-916 for *P. vivax* plasmepsin V were 13.8 and 42.0 nM, respectively, in surface plasmon resonance experiments (**Supplementary Fig. 2a**,**b**). When taken together, our results suggest that WEHI-842 is a more potent inhibitor of *P. falciparum* and *P. vivax* plasmepsin V than is WEHI-916.

WEHI-842 inhibited growth of *P. falciparum* (3D7) parasites, a chloroquine-sensitive strain, with a much higher potency than that of WEHI-916 (**Fig. 1d**). The effect of WEHI-842 on other *P. falciparum* parasites, including chloroquine-resistant strains, was similar to those on 3D7 (**Fig. 1e**). The cytotoxic effect of WEHI-842 and WEHI-916

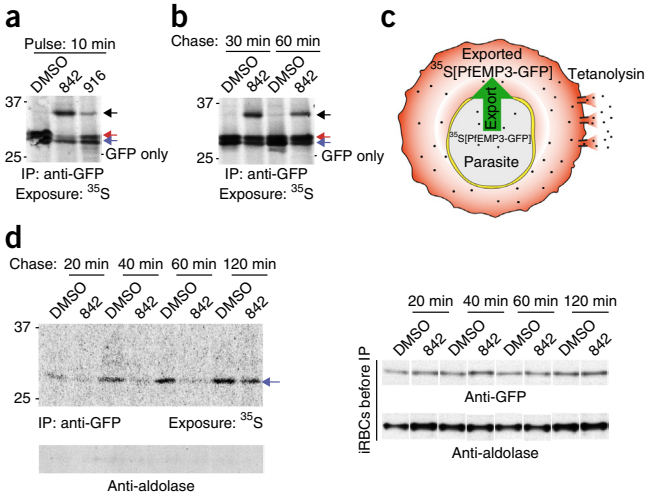

Figure 2 WEHI-842 inhibits cleavage and export of PEXEL proteins to the *P. falciparum*–infected erythrocyte. (**a**) Inhibition of PfEMP3-GFP processing by plasmepsin V with WEHI-842 and WEHI-916 (10 µM). (**b**) Reversible inhibition of PfEMP3-GFP processing by plasmepsin V with WEHI-842. Parasites were treated as in **a** before drug was removed. Black arrow, uncleaved PfEMP3-GFP; red arrow, signal peptidase–cleaved PfEMP3-GFP; blue arrow, PEXEL-cleaved PfEMP3-GFP. (**c**) Schematic showing the assay of soluble proteins exported to the cytosol of *P. falciparum*–infected erythrocytes. (**d**) Blocking of export of PfEMP3-GFP into *P. falciparum*–infected erythrocytes by WEHI-842. Left, PfEMP3-GFP exported to the cytosol of *P. falciparum*–infected erythrocytes over time. Lack of aldolase leakage from the parasite during tetanolysin treatment shown in bottom gel. Right, presence of approximately equal amounts of PfEMP3-GFP and aldolase in treated infected red blood cells (iRBCs) before immunoprecipitation (IP). Each panel in this figure is representative of two independent experiments. Lanes were cropped from different blots. Uncropped images for **a**, **b** and **d** are shown in **Supplementary Data Set 2**.

Table 1 Data collection and refinement statistics

	PMV
Data collection	
Space group	*C*121
Cell dimensions	
a, *b*, *c* (Å)	91.99, 203.09, 82.16
α, β, γ (°)	90, 121.07, 90
Resolution (Å)	41.85–2.368 (2.453–2.368)[a]
R_{merge}	0.1158 (0.6263)
Mean $I / \sigma I$	8.96 (2.07)
Wilson *B* factor (Å^2)	32.34
Completeness (%)	99.22 (98.65)
Redundancy	3.8 (3.7)
Refinement	
Resolution (Å)	41.85–2.368 (2.427–2.368)
No. reflections	51,858 (3,650)
R_{work} / R_{free}	0.1794 (0.2525) / 0.2237 (0.3326)
No. atoms	6,854
Protein	6,402
Ligand/ion	168
Water	284
Average *B* factors (Å^2)	40.20
Protein	39.90
Ligand/ion	52.50
Water	40.20
r.m.s. deviations	
Bond lengths (Å)	0.009
Bond angles (°)	1.16

[a]Values in parentheses are for highest-resolution shell. Ligand/ion represents all nonprotein and nonwater atoms and includes WEHI-842, sulfate, ethylene glycol and jeffamine M-600 molecules. Data were collected from one crystal.

against human HepG2 cells was negligible (half-maximum effective concentration >50 μM). Hence, WEHI-842 is a potent inhibitor of plasmepsin V protease activity *in vitro* and is capable of blocking growth of blood-stage *P. falciparum*.

To determine whether WEHI-842 inhibited processing of PEXEL by plasmepsin V, we used a transfected parasite line expressing an exported protein, *P. falciparum* erythrocyte membrane protein 3 (PfEMP3), containing a PEXEL motif fused to GFP (PfEMP3-GFP) (**Fig. 1f**), and treated the cells with compounds[6] (**Fig. 1g**). WEHI-842 was more potent than WEHI-916 at inhibiting plasmepsin V activity on PfEMP3-GFP expressed in parasites (**Fig. 1g**,**h** and refs. 1,6). The time required to inhibit plasmepsin V was considerably less for WEHI-842 than WEHI-916, requiring 3 h for optimal inhibition compared to 5 h for WEHI-916 (**Fig. 1g**,**h** and ref. 6). In order to provide evidence that WEHI-842 specifically inhibited plasmepsin V and not other normal cellular functions, we showed that the compound did not inhibit parasite translation but potently inhibited plasmepsin V cleavage of PfEMP3-GFP (**Supplementary Fig. 2c**,**d**). Therefore WEHI-842 is a potent and specific inhibitor of plasmepsin V cleavage of the PEXEL in *P. falciparum* parasites.

WEHI-842 inhibits plasmepsin V in infected erythrocytes

To more accurately measure the efficiency of WEHI-842 inhibition of plasmepsin V in *P. falciparum*–infected erythrocytes, we performed pulse-chase experiments (**Fig. 2**). WEHI-842 was more potent than WEHI-916 at inhibiting plasmepsin V–mediated cleavage of the PEXEL in PfEMP3-GFP (**Fig. 2a**). Inhibition of PfEMP3-GFP processing also blocked export of this protein to parasite-infected erythrocytes, as determined with tetanolysin (**Fig. 2c**). Tetanolysin forms pores in parasite-infected erythrocyte membranes, which release the cytosolic contents, thus allowing exported proteins to be assayed (**Fig. 2c**,**d**). Although export in the absence of WEHI-842 was detectable after 20 min and steadily increased after 40, 60 and 120 min, pretreatment with the drug dramatically reduced export. Efficient export of PfEMP3-GFP returned after 120 min of chase, thus demonstrating that inhibition of PEXEL-export by WEHI-842 was reversible (**Fig. 2d**). Therefore WEHI-842 efficiently blocks export of proteins to *P. falciparum*–infected erythrocytes by inhibition of plasmepsin V–mediated cleavage of the PEXEL.

Structure of *P. vivax* plasmepsin V in complex with WEHI-842

To understand how inhibitors inactivate plasmepsin V, we performed crystal screens on apo forms of *P. falciparum* and *P. vivax* proteases in the presence or absence of WEHI-916 and did not obtain well-diffracting crystals. Subsequent use of the high-affinity inhibitor WEHI-842 produced crystals of *P. vivax* enzyme that diffracted to a resolution of 2.37 Å (**Table 1**). The structure revealed a canonical aspartyl protease fold with a crescent shape and a predominantly β-sheet core (**Fig. 3**). The N- and C-terminal subdomains are anchored via a six-stranded interdomain β-sheet (**Fig. 3c**,**d**). A single hairpin loop or 'flap' lies perpendicular over the substrate-binding pocket and interacts with WEHI-842; in this complex, the binding cavity is completely closed. In the *B*-factor putty schematic (**Supplementary Fig. 3a**), we found that most loop regions generally had higher *B* factors, indicating greater flexibility, as expected. However, the flap located over the substrate-binding cavity was relatively well ordered, consistently with its interaction with WEHI-842. *P. vivax* plasmepsin V is predicted to have a predominantly positive surface charge at neutral pH, with substantial patches of negative surface charge associated at one corner of the substrate-binding cavity and another in the vicinity of a helix bundle at the bottom of the molecule (**Supplementary Fig. 3b**).

The loop region between R241 and E272 in *P. vivax* plasmepsin V had poor electron density, and we could not determine its structure. These residues would be located on the opposite side of the molecule from the catalytic cleft, and they presumably don't interact with effector proteins. Plasmepsin V from other *Plasmodium* species also contained regions of similar size at this location, and this loop has poor sequence conservation between species (**Supplementary Fig. 4**). Other Apicomplexa, plant pathogens and plants have enzymes related to plasmepsin V (for example, *Toxoplasma gondii, Theileria orientalis*, *Babesia equi*, *Phytophthora infestans* and *Nepenthes gracilis*), which have sequence identities, similarities and sequence gaps of <35%, <50% and up to 20%, respectively[17]. Other members of the plasmepsin family of aspartyl proteases in *Plasmodium* species (such as plasmepsins II, VI, IX and X) exhibit very low sequence similarity with plasmepsin V, consistently with the unique function of this enzyme in protein export[1,2,18].

The enzyme domain of *P. vivax* plasmepsin V contains 15 cysteine residues forming seven disulfide linkages: four located in the N-terminal subdomain and three in the C-terminal subdomain (**Fig. 4a**). Although *P. vivax* plasmepsin V has a pepsin-like family fold, the disulfide-bond architecture is more complex than in most members within this enzyme group (**Fig. 4a** and ref. 17). Recently, a subfamily of plant aspartic proteases with high cysteine content have been phylogenetically clustered[17]; however, no structural information is available. In this study, we found that plasmepsin V is located within the same clade containing plant and fungal aspartic acid proteases, most of which are type I integral membrane proteins. Our structure for *P. vivax* plasmepsin V, in conjunction with previously

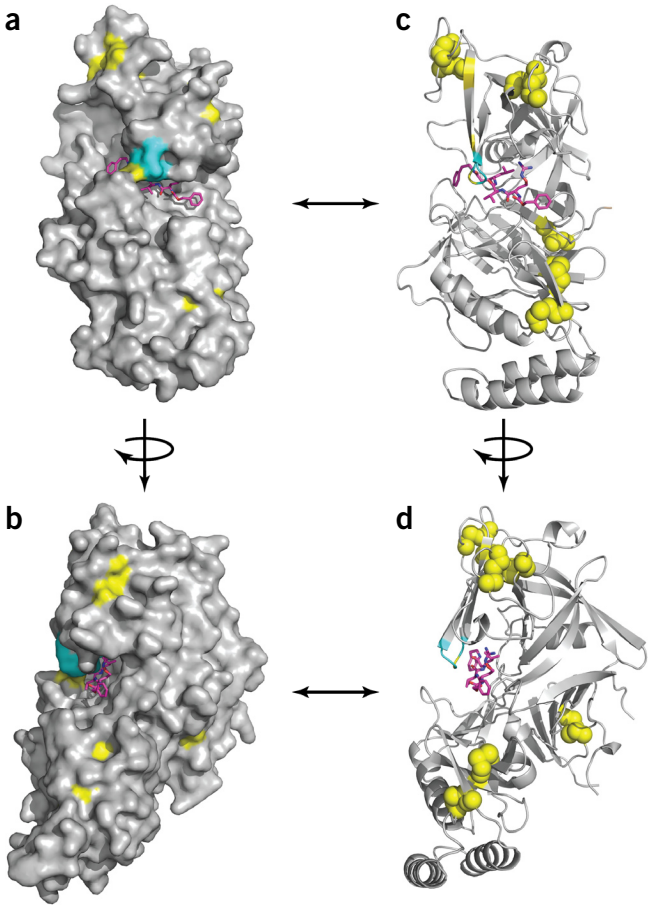

Figure 3 Schematics showing the structure of *P. vivax* plasmepsin V in complex with WEHI-842. (**a**,**b**) Front (**a**) and side (**b**) views in surface representation. (**c**,**d**) Corresponding ribbon diagrams in front (**c**) and side (**d**) views. WEHI-842 (magenta) is bound to the substrate-binding cavity of *P. vivax* plasmepsin V, and the flap (cyan) over the catalytic cleft is in the closed conformation. The free C140 (in the flap) and disulfide-bonded cysteine residues (spheres) are shown in yellow.

reported alignments, suggests a similar disulfide-bond architecture for this group of enzymes and represents the first structure, to our knowledge, for this unusual group of aspartic proteases of subfamily A1B. A C1-C8 disulfide linkage spans the N-terminal subdomain; nestled within this region is a conserved pepsin-like C2-C3 disulfide bond and an insert sequence similar to that found in nepenthesin 1—the 'nepenthesin 1-type' aspartyl protease (NAP1) fold[19]—containing four cysteine residues with disulfide linkages between C4 and C6 and between C5 and C7 (**Supplementary Fig. 5b**). The *P. vivax* plasmepsin V NAP1-insert linkage pattern differs from the C4-C7 and C5-C6 architecture previously predicted from sequence alignments and known structures of pepsin-like aspartic proteases[17,19]. We did not observe the unpaired cysteine residue (C7a), located adjacent to the archetypal tyrosine in the flap, above the substrate-binding site in other Apicomplexans or in closely related plant and fungal aspartic proteases, and it therefore appears to be unique to *Plasmodium* species (**Supplementary Fig. 5c**).

A sequence and secondary-structural alignment between *P. vivax* plasmepsin V and *P. falciparum* plasmepsin II (a member of the plasmepsin family involved in hemoglobin digestion) shows low sequence homology but a high level of preservation of secondary-structural elements throughout the enzyme domains (**Supplementary Fig. 5a**). Alignment of both structures (**Fig. 4b**) showed good conservation of the fold within the core and cleft regions, as can be visualized when the aligned structures are colored according to r.m.s. deviation (**Fig. 4b**,**c**). The structural similarity decreases toward the extremities, where more-mobile regions or structural differences such as the NAP1 insert and helix-turn-helix occur (**Fig. 4b**). In *P. vivax* plasmepsin V, the NAP1 insert forms a surface loop (Y116–G121) (**Fig. 4b** and ref. 19), a feature not present in *P. falciparum* plasmepsin II. There were also minor changes in the alignment of other structural elements in the vicinity of the inserted loop (**Fig. 4c**). The NAP1 insert is not in other members of the broader plasmepsin family such as plasmepsins VI, IX and X. Intriguingly, the flap that sits above the substrate-binding site in *P. vivax* plasmepsin V appears to be associated with the NAP1 insert. The flap sequence, which contains the unpaired C140, is highly conserved in orthologs of plasmepsin V in *Plasmodium* species (**Supplementary Fig. 5b**). One of the disulfide bonds (i.e., C5-C7) within the NAP1 insert tethers this loop to the N-terminal β-strand within the flap. The NAP1 insert has been suggested to have a role in functional regulation of nepenthesin 1 (ref. 19). The *P. vivax* plasmepsin V structure suggests that the flap may be influenced by an interaction with another protein through the NAP1 insert. Primary candidates would be PEXEL effectors, because they enter to dock for processing and require the flap to be sufficiently open for the PEXEL motif of a large polypeptide to insert into the catalytic cleft (**Supplementary Fig. 5c**,**d**). Sequence alignments of plasmepsin V indicate that this proposed 'molecular gate' for PEXEL access could be conserved throughout Apicomplexa and related plant and fungal enzymes (**Supplementary Fig. 5c**,**d**). Although we did not include the short prosequence for *P. vivax* plasmepsin V in structure determination, its location has been predicted to be oriented away from the catalytic-cleft region, thus leaving this enzyme in a continuous active state[1,2,12].

The helix-turn-helix motif is another key feature of *P. vivax* plasmepsin V and is conserved only within orthologs of *Plasmodium* species (**Supplementary Fig. 4**). The helix-turn-helix motif (**Fig. 4b**) is also absent from other crystalized plasmepsins, including *P. falciparum* plasmepsin II. An overlay shows that their structures align poorly in the regions N terminal (helix 5) and C terminal (the β-sheet incorporating the β15a strand) to the C337-C382 (C10-C11) tethering point in *P. vivax* plasmepsin V (**Fig. 4a**,**b**). This can be explained by the way the helix-turn-helix motif is stabilized internally and within the adjoining areas of the plasmepsin V molecule. These amphipathic helices are held strongly together in an antiparallel orientation by hydrophobic residues oriented toward each other along the internal face of the motif while the β15a strand is involved in the disulfide-bond tethering of the motif. The hydrophilic residues lining the outside edges of the helix-turn-helix motif are highly conserved in plasmepsin V orthologs across *Plasmodium* species (**Supplementary Fig. 5a**). The conservation of this structural element and surrounding features suggests their important functional roles.

P. vivax plasmepsin V interaction with WEHI-842

The N-terminal benzyl carbamate moiety of WEHI-842 protrudes outside the cleft and does not directly influence the binding affinity of the inhibitor (**Fig. 5a** and refs. 13,16). Consistently with those of other protease inhibitors, the protein-ligand interactions primarily involve residues in proximity to the two catalytic aspartate residues and those located in the flap directly above the substrate-binding cleft[20–22]. As expected, the two catalytic aspartate residues of plasmepsin V interacted with the statine hydroxyl functionality, which mimics the transitional-state intermediate formed during the

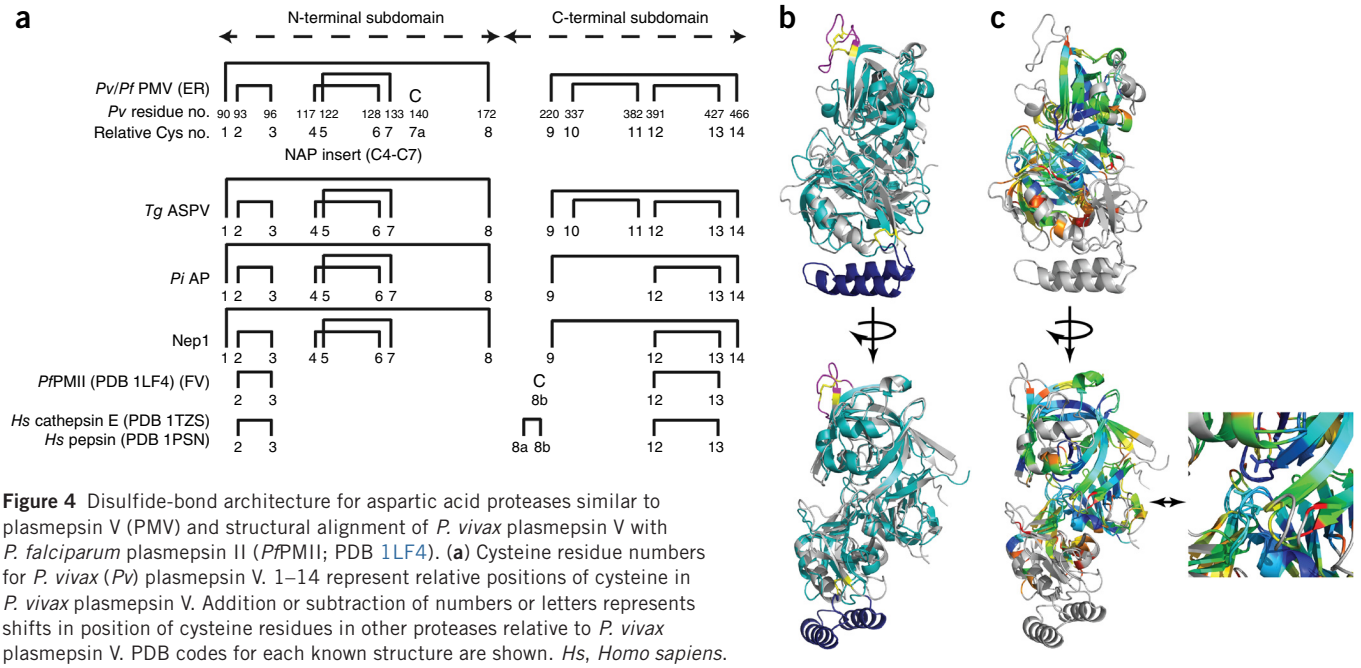

Figure 4 Disulfide-bond architecture for aspartic acid proteases similar to plasmepsin V (PMV) and structural alignment of *P. vivax* plasmepsin V with *P. falciparum* plasmepsin II (*Pf*PMII; PDB 1LF4). (**a**) Cysteine residue numbers for *P. vivax* (*Pv*) plasmepsin V. 1–14 represent relative positions of cysteine in *P. vivax* plasmepsin V. Addition or subtraction of numbers or letters represents shifts in position of cysteine residues in other proteases relative to *P. vivax* plasmepsin V. PDB codes for each known structure are shown. *Hs*, *Homo sapiens*. Plasmepsin II is located in the food vacuole (FV).The disulfide connectivity for *P. falciparum (Pf)* PMV, *T. gondii* (*Tg*) ASPV, *Phytophthora infestans* (*Pi*) AP12 (XP_002901082.1) and *N. gracilis* Nep1 are predicted according to structure-alignment models. (**b**) Schematic of the aligned structures for *P. vivax* plasmepsin V and *P. falciparum* plasmepsin II. The top view is of the front of the substrate-binding cleft; the bottom view is a 90°-clockwise rotation showing a side view into the substrate-binding cleft. The NAP1 insert sequence (magenta) in *P. vivax* plasmepsin V is located toward the top of the structure, and the helix-turn-helix region (dark blue) is on the bottom edge. Disulfide bonds in both of these structural elements are shown in yellow. (**c**) *P. vivax* plasmepsin V and *P. falciparum* plasmepsin II, aligned and colored by r.m.s. deviation (which measures distances in Å between the Cα atoms of two aligned residues). Dark-blue coloring represents good alignment, whereas higher deviations are shown progressively through green to red. Residues not aligned are colored white. The level of structural similarity of the substrate-binding cleft is shown in the inset.

cleavage of the peptide bond; these interactions explain the mechanism of plasmepsin V inhibition by WEHI-842.

The oxo-guanidinium ion of WEHI-842 lies deep within the S_3 pocket of plasmepsin V and participates in multiple interactions that anchor it to the substrate-binding cleft (**Fig. 5b**). The carboxylic acid moiety of E141 of the plasmepsin V flap forms a 'side-on' salt bridge with the guanidinium ion while the carbonyl group on the Q183 side chain interacts with two hydrogen atoms located at the distal end of the same ion (**Fig. 5a–c**). The guanidinium ion is further stabilized via hydrogen-bonding to a water molecule (H_2O no. 2 in **Fig. 5a**) that also interacts with the main chain carbonyl of Y59. Interestingly, the aspartyl protease penicillopepsin (PDB 3APP[24], Merops database), which contains an aspartate in place of E141 in its flap, appears to be highly specific for lysine in the P_3 position of its substrate, and thus the flap of plasmepsin V may help influence substrate specificity. These interactions of the guanidine side chain explain why the PEXEL arginine is important for plasmepsin V activity.

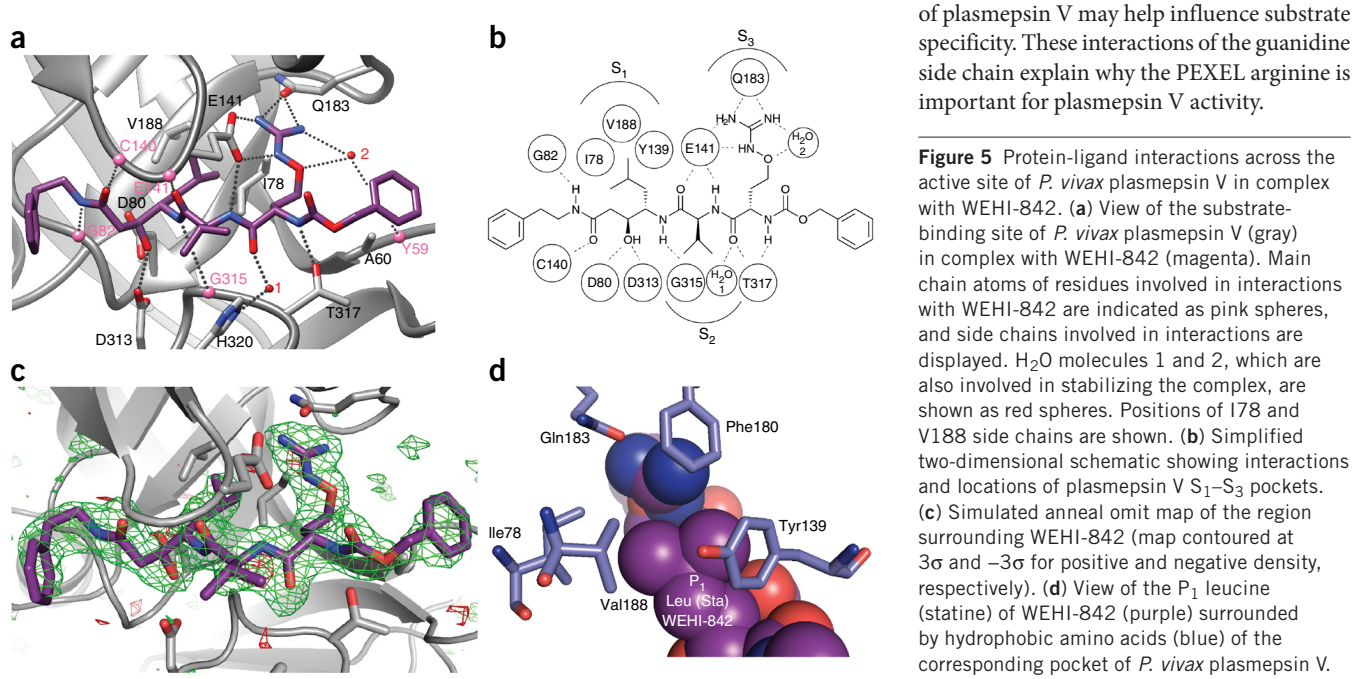

Figure 5 Protein-ligand interactions across the active site of *P. vivax* plasmepsin V in complex with WEHI-842. (**a**) View of the substrate-binding site of *P. vivax* plasmepsin V (gray) in complex with WEHI-842 (magenta). Main chain atoms of residues involved in interactions with WEHI-842 are indicated as pink spheres, and side chains involved in interactions are displayed. H_2O molecules 1 and 2, which are also involved in stabilizing the complex, are shown as red spheres. Positions of I78 and V188 side chains are shown. (**b**) Simplified two-dimensional schematic showing interactions and locations of plasmepsin V S_1–S_3 pockets. (**c**) Simulated anneal omit map of the region surrounding WEHI-842 (map contoured at 3σ and –3σ for positive and negative density, respectively). (**d**) View of the P_1 leucine (statine) of WEHI-842 (purple) surrounded by hydrophobic amino acids (blue) of the corresponding pocket of *P. vivax* plasmepsin V.

The P_1 leucine in the PEXEL has been shown to be important for binding affinity of plasmepsin V substrates and inhibitors[6,16,23]. Our structure reveals that this residue occupies the S_1 pocket and is tightly encapsulated within the hydrophobic environment created by the juxtaposition of I78, Y139 and V188 (**Fig. 5d**). Hence, even substitution by the structural isomer isoleucine has limited tolerance[6,16,23]. The majority of carbonyl and amide groups along the length of WEHI-842 are involved in hydrogen-bonding with surrounding amino acids and solvent molecules (for example, H_2O no. 1 in **Fig. 5a**), thus creating an extensive network of interactions anchoring the inhibitor across the substrate-binding cavity (**Fig. 5a–c**). The unpaired C140 residue in the flap above the substrate-binding cleft interacts, via its main chain amide group, with the statine carbonyl on WEHI-842. Although the C140 side chain orients toward the inhibitor, there was no obvious interaction for the thiol; this group is quite reactive and could potentially be exploited in the design of inhibitors.

In alignments of orthologs of *Plasmodium* species, the residues lining the surface of the substrate binding cavity are essentially identical except for two alternative residues in the S_5 position for *P. falciparum*, *Plasmodium vinckei* and *Plasmodium berghei* plasmepsin V (not shown). Such high levels of conservation indicate that high-affinity inhibitors identified for plasmepsin V should be effective against most if not all *Plasmodium* species and suggest that animal models can be used for *in vivo* kinetic studies. The cavity surface for the orthologs from other Apicomplexa and nepenthesin 1 show variations in sequence around some of the key interactive residues and various substrate-binding pockets throughout the cavity, thus suggesting that inhibitors optimized for use against *Plasmodium* species may not be as active against other related aspartyl proteases.

Analysis of the enzyme–inhibitor structure reveals that not all cavity space has been utilized in this complex. The ability for naturally occurring peptides to efficiently fill this space may be limited, whereas non-peptide-based inhibitors may offer a greater scope in geometry and physicochemical properties, which could lead to improved affinities for plasmepsin V. For example, the P_2 position on WEHI-842 is optimal for valine, but isoleucine and leucine can be tolerated in this position with minimal changes to affinity[16]. It is apparent that the S_2 pocket is only partially filled by the valine residue of WEHI-842. Furthermore, the main cavity of the P_3 pocket is largely filled by the canavanine side chain; however, a smaller yet equally deep cavity also exists on the floor of this pocket and is not utilized by this inhibitor. Finally, the pockets on the edge of the substrate binding cavity, such as S_1', S_2', S_4 and S_5 may offer additional opportunities to improve the affinities of future inhibitors to plasmepsin V.

DISCUSSION

Plasmepsin V acts at the first step in export of PEXEL proteins and is essential for *P. falciparum* survival; thus, it is a potential drug target for development of new antimalarials[1,2,6]. WEHI-842 potently inhibits plasmepsin V protease activity and protein export and has lethal effects on *P. falciparum* growth. In this study we have obtained a three-dimensional structure of WEHI-842–bound plasmepsin V. This structure allows for insights into the active site as well as identification of unique structural domains likely to be important for export function.

WEHI-842 and WEHI-916 mimic the transition state of amide-bond proteolysis for PEXEL substrates[6]. WEHI-916 is a good inhibitor of plasmepsin V, but it is not potent in blocking *P. falciparum* growth. This is probably because the guanidinium group on the P_3 arginine impairs permeability across membranes. WEHI-842 has a non-proteinogenic amino acid, canavanine, replacing the P_3 arginine and has an N-terminal carbamate instead of the sulfonamide in WEHI-916. Consequently, WEHI-842 is a more potent inhibitor of plasmepsin V and *P. falciparum* growth. The exchange of sulfonamide with a carbamate has been shown to have no effect on binding affinity to plasmepsin V or parasite activity[13], so the improvement that we observed with WEHI-842 was due to replacement of the P_3 arginine with canavanine. It is likely that WEHI-842 is a better inhibitor of plasmepsin V because the oxo-guanidinium moiety interacts with a water molecule—an interaction that WEHI-916 cannot establish. This would further stabilize the interaction of P_3 canavanine with amino acids in the S_3 pocket of plasmepsin V. Additionally, the replacement of the carbon in WEHI-916 with oxygen in WEHI-842 may exert a slight change in bond angle that is more beneficial for binding. Furthermore, this oxygen alters the basicity or pK_a of the guanidine[25], thus causing better membrane permeability and overall improvement in WEHI-842 temporal and antiparasitic activity.

WEHI-842 mimics the RVL amino acid sequence of PEXEL, and its structure in the plasmepsin V pocket provides insights into the RxL substrate preference of the enzyme. The PEXEL P_3 arginine differs from the corresponding region of WEHI-842 in the oxygen adjacent to the guanidinium ion, which is replaced by a carbon. It is unlikely that any other amino acid would be accepted in the P_3 position and form such an intricate network of hydrogen bonds in the S_3 pocket of plasmepsin V. Lysine is poorly tolerated in the P_3 position because plasmepsin V has greatly reduced activity for these substrates (**Supplementary Fig. 1** and refs. 6,16,23). Furthermore, PEXEL mimetics containing lysine are poor inhibitors of plasmepsin V[16]. However, our analyses of substrate specificity focused on the PEXEL from KAHRP (RTLAQ) or mimetics of the PEXEL sequences RVL and RAL. Recently, it has been shown that both histidine and lysine in the P_3 position of noncanonical PEXEL sequences are processed and exported in parasites but not in the context of the KAHRP sequence[26]. Our structure does not provide an obvious explanation for why KQLSE but not KTLAQ might be cleaved by plasmepsin V; however, structural differences imparted by different residues of the PEXEL may be involved. Plasmepsin V has a preference for leucine at the P_1 position of the PEXEL, and it inefficiently cleaves KAHRP substrates containing isoleucine at P_1 (**Supplementary Fig. 1** and refs. 6,16,23). In plasmepsin V, the P_1 leucine is tightly packed with several hydrophobic residues in the S_1 pocket, but it is plausible that in a dynamic environment a similar residue such as isoleucine may be tolerated. Indeed, we have shown that a peptidomimetic with a P_1 isoleucine (WEHI-025) possesses some, albeit weak, affinity for *P. falciparum* and *P. vivax* plasmepsin V[6]. This suggests that the hydrophobic S_1 pocket weakly accommodates a P_1 isoleucine. Therefore, although there is strong evidence that plasmepsin V has an overwhelming preference for the RxL motif, the parasite may use substrate sequences with lower-than-maximum affinity for plasmepsin V for export.

Sequence alignments suggest that the structure of *P. vivax* plasmepsin V may be highly conserved across *Plasmodium* species. However, although plasmepsin V–like aspartyl proteases in other Apicomplexa and related plant and fungal enzymes have the core fold, and in some cases have part of the NAP1 insert, they do not have the helix-turn-helix motif found in the *P. vivax* enzyme. This is probably because of the different functions of these enzymes and the environments in which they reside[27]. The helix–turn-helix motif is unique to plasmepsin V from *Plasmodium* species; it is highly conserved, and, although its function is unknown, we suspect that it is involved in protein-protein interactions required for the enzyme's function in the ER. The NAP1 insert, from plant aspartyl proteases, has been identified previously, but the structure for *P. vivax* plasmepsin V

reveals that it associates with the flap on the outside of the active site. It could potentially form a molecular gate restricting access to the catalytic cleft until a PEXEL protein interacts with the NAP1 insert, thus resulting in a conformational change allowing the flap to open (**Supplementary Fig. 5**).

Identification of the residues lining the catalytic cleft in *P. vivax* plasmepsin V and comparison to the equivalent residues in alignments of plasmepsin V orthologs in *Plasmodium* species indicate that the catalytic cleft is highly conserved. Given the essential nature of this enzyme and its relative evolutionary distance from mammalian aspartyl proteases, this conservation of plasmepsin V in rodent species of malaria parasites could provide a unique opportunity to perform *in vivo* studies of inhibitor kinetics in animal models, with the goal of optimization of therapies for treatment of malaria in humans. Furthermore, the structure provides insight into strategies that could be used to improve future inhibitors of this enzyme and to design inhibitors against other parasite, plant and fungal homologs of plasmepsin V.

METHODS

Methods and any associated references are available in the online version of the paper.

Accession codes. Coordinates and structure factors for *P. vivax* plasmepsin V have been deposited in the Protein Data Bank under accession code 4ZL4.

Note: Any Supplementary Information and Source Data files are available in the online version of the paper.

ACKNOWLEDGMENTS

We thank the Red Cross Blood Service (Melbourne, Australia) for supply of blood and the Australian Synchrotron and Commonwealth Scientific and Industrial Research Organisation Crystallization Facility. This work was supported by the Victorian State Government Operational Infrastructure Support and Australian Government National Health and Medical Research Council (NHMRC) Independent Research Institute Infrastructure Support Scheme, the Australian Cancer Research Foundation and the NHMRC (grants 1057960 (A.F.C.), 637406 (A.F.C.) and 1010326 (J.A.B.)). We thank the University of Melbourne for the provision of an Australian Postgraduate Award to M.G. A.F.C. is supported as a Howard Hughes International Scholar, P.E.C. is supported as an National Health and Medical Research Council of Australia Senior Research Fellow, and J.A.B. is supported as an Australian Research Council Queen Elizabeth II Fellow. We thank G. Lessene for useful discussions and Jacobus Pharmaceuticals for providing WR99210.

AUTHOR CONTRIBUTIONS

A.N.H., B.E.S., J.A.B. and A.F.C. designed the experiments and wrote the manuscript. A.N.H. expressed, characterized, purified and crystallized plasmepsin V. B.E.S. and M.G. designed and synthesized WEHI-842. T.T. provided expert advice and supervision with respect to the molecular biology. P.E.C. collected X-ray data and solved and built the structure. P.E.C., A.N.H., B.J.S. and Y.X. did structural analysis of plasmepsin V with bound WEHI-842. B.J.S. and A.N.H. obtained enzyme kinetic data. M.T.O'N., S.L. and J.A.B. obtained biological data on the effect of WEHI-824. K.L. obtained surface plasmon resonance data. T.N. performed and analyzed proteomic experiments.

COMPETING FINANCIAL INTERESTS

The authors declare no competing financial interests.

1. Boddey, J.A. *et al.* An aspartyl protease directs malaria effector proteins to the host cell. *Nature* **463**, 627–631 (2010).
2. Russo, I. *et al.* Plasmepsin V licenses *Plasmodium* proteins for export into the host erythrocyte. *Nature* **463**, 632–636 (2010).
3. Marti, M., Good, R.T., Rug, M., Knuepfer, E. & Cowman, A.F. Targeting malaria virulence and remodeling proteins to the host erythrocyte. *Science* **306**, 1930–1933 (2004).
4. Hiller, N.L. *et al.* A host-targeting signal in virulence proteins reveals a secretome in malarial infection. *Science* **306**, 1934–1937 (2004).
5. Boddey, J.A. & Cowman, A.F. *Plasmodium* nesting: remaking the erythrocyte from the inside out. *Annu. Rev. Microbiol.* **67**, 243–269 (2013).
6. Sleebs, B.E. *et al.* Inhibition of Plasmepsin V activity demonstrates its essential role in protein export, PfEMP1 display, and survival of malaria parasites. *PLoS Biol.* **12**, e1001897 (2014).
7. Chang, H.H. *et al.* N-terminal processing of proteins exported by malaria parasites. *Mol. Biochem. Parasitol.* **160**, 107–115 (2008).
8. Boddey, J.A., Moritz, R.L., Simpson, R.J. & Cowman, A.F. Role of the *Plasmodium* export element in trafficking parasite proteins to the infected erythrocyte. *Traffic* **10**, 285–299 (2009).
9. Sargeant, T.J. *et al.* Lineage-specific expansion of proteins exported to erythrocytes in malaria parasites. *Genome Biol.* **7**, R12 (2006).
10. Elsworth, B. *et al.* PTEX is an essential nexus for protein export in malaria parasites. *Nature* **511**, 587–591 (2014).
11. Beck, J.R., Muralidharan, V., Oksman, A. & Goldberg, D.E. PTEX component HSP101 mediates export of diverse malaria effectors into host erythrocytes. *Nature* **511**, 592–595 (2014).
12. Klemba, M. & Goldberg, D.E. Characterization of plasmepsin V, a membrane-bound aspartic protease homolog in the endoplasmic reticulum of *Plasmodium falciparum*. *Mol. Biochem. Parasitol.* **143**, 183–191 (2005).
13. Gazdik, M. *et al.* The effect of N-methylation on transition state mimetic inhibitors of the *Plasmodium* protease, plasmepsin V. *Med. Chem. Commun.* **6**, 437–443 (2015).
14. Masic, L.P. Arginine mimetic structures in biologically active antagonists and inhibitors. *Curr. Med. Chem.* **13**, 3627–3648 (2006).
15. Peterlin-Mašič, L. & Kikelj, D. Arginine mimetics. *Tetrahedron* **57**, 7073–7105 (2001).
16. Sleebs, B.E. *et al.* Transition state mimetics of the *Plasmodium* export element are potent inhibitors of Plasmepsin V from *P. falciparum* and *P. vivax*. *J. Med. Chem.* **57**, 7644–7662 (2014).
17. Kay, J., Meijer, H.J., ten Have, A. & van Kan, J.A. The aspartic proteinase family of three *Phytophthora* species. *BMC Genomics* **12**, 254 (2011).
18. Meyers, M.J. & Goldberg, D.E. Recent advances in plasmepsin medicinal chemistry and implications for future antimalarial drug discovery efforts. *Curr. Top. Med. Chem.* **12**, 445–455 (2012).
19. Athauda, S.B. *et al.* Enzymic and structural characterization of nepenthesin, a unique member of a novel subfamily of aspartic proteinases. *Biochem. J.* **381**, 295–306 (2004).
20. Haque, T.S. *et al.* Potent, low-molecular-weight non-peptide inhibitors of malarial aspartyl protease plasmepsin II. *J. Med. Chem.* **42**, 1428–1440 (1999).
21. Ghosh, A.K. *et al.* Structure-based design: Potent inhibitors of human brain memapsin 2 (β-secretase). *J. Med. Chem.* **44**, 2865–2868 (2001).
22. Johansson, P.-O. *et al.* Design and synthesis of potent inhibitors of plasmepsin I and II: X-ray crystal structure of inhibitor in complex with plasmepsin II. *J. Med. Chem.* **48**, 4400–4409 (2005).
23. Boddey, J.A. *et al.* Role of Plasmepsin V in export of diverse protein families from the *Plasmodium falciparum* exportome. *Traffic* **14**, 532–550 (2013).
24. James, M.N. & Sielecki, A.R. Structure and refinement of penicillopepsin at 1.8 A resolution. *J. Mol. Biol.* **163**, 299–361 (1983).
25. Meanwell, N.A. Synopsis of some recent tactical application of bioisosteres in drug design. *J. Med. Chem.* **54**, 2529–2591 (2011).
26. Schulze, J. *et al.* The *Plasmodium falciparum* exportome contains non-canonical PEXEL/HT proteins. *Mol. Microbiol.* doi:10.1111/mmi.13024 (9 May 2015).
27. Shea, M. *et al.* A family of aspartic proteases and a novel, dynamic and cell-cycle-dependent protease localization in the secretory pathway of *Toxoplasma gondii*. *Traffic* **8**, 1018–1034 (2007).

ONLINE METHODS

Synthesis of WEHI-842. The chemistry, scheme and methods for synthesis of WEHI-842 are described in the **Supplementary Note**.

Protein expression and purification. *P. vivax* plasmepsin V (residues R35–R476), bearing an N-terminal gp67 signal peptide and a fusion tag comprising a FLAG tag, SUMO domain and tobacco etch virus (TEV) protease-cleavage site, was expressed in High Five insect cells. Recombinant protein was purified initially from cell supernatant with anti-FLAG M2-agarose (Sigma). Pooled fractions were concentrated, and the N-terminal fusion tag was removed with TEV protease (1:25 (v/v), 5 h, room temperature). Gel-filtration chromatography (Superdex 75, GE Life Sciences) in 20 mM HEPES, pH 7.2, 100 mM NaCl, and 0.2 mM DTT resulted in pure and stable protein that was concentrated for crystallization. A similar procedure was used for the production of *P. falciparum* plasmepsin V (residues N80–R528), except that sf21 insect cells were used for protein expression because less covalent aggregate was observed to be produced in this cell system.

Kinetic characterization of recombinant plasmepsin V. The activity of recombinant *P. falciparum* and *P. vivax* plasmepsin V was assessed against the KAHRP fluorogenic peptide (DABCYL-RNKRTLAQKQ-E-EDANS). Values for K_m were derived from both the inverse Michaelis-Menten and the Lineweaver-Burk plots. These values were of the same magnitude for each enzyme and are also similar to the K_m values derived from the activity of another recombinant form of *P. falciparum* plasmepsin V on a different PEXEL substrate[28].

Biochemical assays. PEXEL cleavage assays (20 µl total volume) consisted of 1 ng per well of *P. vivax* plasmepsin V or 1.5 ng per well of *P. falciparum* plasmepsin V in buffer (25 mM Tris-HCl and 25 mM MES, pH 6.4) with 5 µM FRET peptide substrate (DABCYL-RNKRTLAQKQ-E-EDANS or peptides with the sequence DABCYL-RNKKTLAQKQ-E-EDANS or DABCYL-RNKRTIAQKQ-E-EDANS) (ChinaPeptides)[6]. Samples were incubated at 37 °C for 120 min and were measured with an Envision plate (PerkinElmer) reader (ex, 340 nm; em, 490 nm).

Compound evaluation. Compounds WEHI-916 and WEHI-842 were evaluated with the fluorogenic PEXEL cleavage assays described above[6]. Reactions included a fluorescent peptide of nine amino acids containing the PEXEL sequence (RTLAQ) from KAHRP[1]. The KAHRP PEXEL peptide substrate DABCYL-RNKRTLAQKQ-E-EDANS (ChinaPeptides) was obtained commercially and was used at a final assay concentration of 7.5 µM. The endpoint for all assays was set within the linear range of activity (approximately 1 h). Tween-20 was used at 0.005% final assay concentration. The final assay buffer concentration was as follows: 25 mM Tris HCl and 25 mM MES, pH 6.4 (ref. 1). The final assay volume was 20 µl. A ten-point 1-in-3 serial dilution of compounds was generated with DMSO as a diluent (final assay concentration of 1%). Assay reactions were incubated for 30 min at 37 °C and read with a fluorescence plate reader (ex, 340 nm; em, 495 nm). IC_{50} values were determined with a nonlinear regression four-parameter fit analysis in which the parameters were not constrained. The equation used in GraphPad Prism (version 6.05) is sigmoidal dose response (variable slope). The equation used was $Y = \text{bottom} + (\text{top} - \text{bottom})/(1+10^{((\log EC50 - X)\times \text{Hill Slope})})$.

Parasites and growth assays. *P. falciparum* strains 3D7 (D. Walliker, Edinburgh University), NF54 (Walter Reed Army Institute of Research), CS2 (CSL Limited) and W2mef (Malaria Research and Reference Reagent Resource Centre, MR4) were cultured in human O^+ erythrocytes at 4% hematocrit in RPMI 1640 medium containing 25 mM HEPES, pH 7.4, 0.2% sodium bicarbonate, 0.5% Albumax II (Life Technologies) and 5 nM WR99210 for selection where required (a gift from Jacobus Pharmaceuticals) in 5% CO_2, 5% O_2, 90% N at 37 °C. *P. falciparum* 3D7 expressing PfEMP3-GFP were as generated previously[1]. Use and supply of human red blood cells from the Australian Red Cross (supply agreement 13-08VIC) has been approved by the Walter and Eliza Hall Institute of Medical Research Human Research Ethics Committee (HREC86,17). The blood used for culturing *P. falciparum* parasites was obtained from human volunteers by the Australian Red Cross, who obtain informed consent. The blood was supplied to us deidentified. Growth assays were performed in 96-well plates by incubating ring-stage *P. falciparum* parasites with WEHI-916 or WEHI-842 solubilized in DMSO (maximum 0.1% final concentration), or chloroquine solubilized in water, at the indicated concentrations, and parasitemia was determined at 72 h by flow cytometry as described previously[6]. Parasite lines have been periodically tested for mycoplasma contamination, and identity was authenticated by whole-genome sequencing and by the drug-resistance and sensitivity phenotypes expected.

Immunoblots, pulse chase and densitometry. *P. falciparum* trophozoites expressing PfEMP3-GFP were magnet-purified (Miltenyi Biotech), incubated with inhibitors for 1–4 h at 37 °C, and treated with 0.09% saponin-containing inhibitor. Washed pellets were solubilized in Laemmli buffer and boiled for 3 min, and proteins were separated by SDS-PAGE, transferred to nitrocellulose and blocked in 1% skim milk. Membranes were probed with mouse anti-GFP (Roche, cat. no. 11814460001) (1:1,000) (primary validation is provided on the manufacturer's website), rabbit anti-aldolase (1:1,000)[29] or rabbit anti-HSP70 (1:4,000)[30]; this was followed by probing with horseradish peroxidase–conjugated secondary antibodies (Cell Signaling Technology, cat. nos. 7074, 7076 and 7077) and visualization with enhanced chemiluminescence (Amersham). To radiolabel *P. falciparum* proteins, magnet-purified trophozoites expressing PfEMP3-GFP were treated with 10 µM inhibitors for 3 h (with the final 30 min in methionine- and cysteine-free medium) at 37 °C before addition of 800 µCi/ml ^{35}S-labeled methionine and cysteine (PerkinElmer) to the medium for 10 min. PfEMP3-GFP protein species were then immunoprecipitated from parasite lysates solubilized in 1% Triton X-100, PBS containing 1× Complete protease inhibitors (Roche) with anti-GFP agarose (MBL, D153-8) for 2 h at 4 °C, and proteins were resolved by SDS-PAGE, visualized by autoradiography and quantified with a GS-800 Calibrated Densitometer (Bio-Rad)[6]. Pulse chases were performed by radiolabeling of proteins as above, before further culture in radiolabel-free, inhibitor-free complete medium for 30 and 60 min at 37 °C before PfEMP3-GFP protein species were purified, resolved, visualized and quantified by densitometry, as above.

Pulse chases to measure protein export and inhibition. For the pulse, *P. falciparum* trophozoites expressing PfEMP3-GFP were magnet-purified (Miltenyi Biotech) and treated with 10 µM WEHI-842 or DMSO for 3 h. Parasite proteins were labeled in the presence of inhibitors by addition of 800 µCi/ml ^{35}S-labeled methionine and cysteine (PerkinElmer) to the medium for the last 50 min of the 3-h inhibitor treatment (this included 30 min in methionine- and cysteine-free medium containing inhibitor before labeling). Then export of labeled proteins to the erythrocyte was chased by culturing parasites in radiolabel-free, inhibitor-free complete medium for either 20, 40, 60 or 120 min at 37 °C in culture gas before exported proteins were liberated from the infected erythrocytes by tetanolysin treatment (100 U/mL tetanolysin (Sigma), 0.2% bovine serum albumin (Sigma), and 1× Complete protease-inhibitor cocktail (Roche)) for 5 min at 37 °C and centrifugation at 1,500*g* for 1 min. PfEMP3-GFP proteins were purified from the tetanolysin supernatant fraction with anti-GFP agarose and resolved, visualized and quantified by densitometry, as above.

Surface plasmon resonance. Surface plasmon resonance was performed with a Biacore 4000 (GE Healthcare). *P. vivax* plasmepsin V was immobilized on a Series S CM5 sensor chip with amine-coupling chemistry. The surfaces of flow cells were activated for 10 min with a 1:1 mixture of 0.1 M NHS (*N*-hydroxysuccinimide) and 0.1 M EDC (3-(*N*,*N*-dimethylamino)propyl-*N*-ethylcarbodiimide) at a flow rate of 5 µl/min. Plasmepsin V (20 µg/ml in 10 mM sodium acetate, pH 4.5, was immobilized at a density of approximately 10,000. Spot 3 was activated and deactivated as above and used as a reference surface. All surfaces were blocked with a 7-min injection of 1 M ethanolamine, pH 8.0. WEHI-916 and WEHI-842 ten-point titrations were prepared by 1:2 dilution from 1,000 nM and injected at a flow rate of 30 µl/min. The buffer used was 10 mM HEPES, 150 mM NaCl, 3 mM EDTA, 0.05% Tween and 2% DMSO. Analysis was performed at 25 °C. After compound injection, the chip surface was regenerated with 10 mM glycine-HCl, pH 2 for 30 s. Compounds were allowed to associate and dissociate for 250 s and 600 s, respectively. Data were collected at a rate of 10 Hz and fit to a 1:1 interaction model with Biacore 4000 Evaluation Software Version 1.0.

Structure determination. *P. vivax* plasmepsin V (8 mg/ml) was cocrystallized with WEHI-842 (6× molar excess) in 0.11 M ammonium sulfate, 5% (v/v) jeffamine M-600, 15.5% (w/v) polyethylene glycol 4000, and 0.1 M sodium

doi:10.1038/nsmb.3061

acetate-acetic acid, pH 4.16, and crystals were frozen in well solution supplemented with 20% ethylene glycol. Data were collected at the Australian Synchrotron beamline MX2 at 100 K and processed with XDS[31,32], Pointless[32] and Aimless[33]. The structure was solved by molecular replacement with Phaser[34] with a Sculptor[35]-modified version of cathepsin E (PDB 1TZS[36]) as the search model. Further rounds of building and refinement with Coot[37] and Phenix[38] yielded the final model. Patches of poorly defined density connected residues R241–E272 but were of inadequate quality for model building with confidence. Density observed proximal to Asn355 may be due to glycosylation of this residue during protein expression.

28. Xiao, H. *et al.* The zymogen of plasmepsin V from *Plasmodium falciparum* is enzymatically active. *Mol. Biochem. Parasitol.* **197**, 56–63 (2014).
29. Baum, J. *et al.* A conserved molecular motor drives cell invasion and gliding motility across malaria life cycle stages and other apicomplexan parasites. *J. Biol. Chem.* **281**, 5197–5208 (2006).
30. Bianco, A.E. *et al.* A repetitive antigen of *Plasmodium falciparum* that is homologous to heat shock protein 70 of *Drosophila melanogaster*. *Proc. Natl. Acad. Sci. USA* **83**, 8713–8717 (1986).
31. Kabsch, W. XDS. *Acta Crystallogr. D Biol. Crystallogr.* **66**, 125–132 (2010).
32. Evans, P.R. An introduction to data reduction: space-group determination, scaling and intensity statistics. *Acta Crystallogr. D Biol. Crystallogr.* **67**, 282–292 (2011).
33. Evans, P.R. & Murshudov, G.N. How good are my data and what is the resolution? *Acta Crystallogr. D Biol. Crystallogr.* **69**, 1204–1214 (2013).
34. McCoy, A.J. *et al.* Phaser crystallographic software. *J. Appl. Crystallogr.* **40**, 658–674 (2007).
35. Bunkóczi, G. & Read, R.J. Improvement of molecular-replacement models with Sculptor. *Acta Crystallogr. D Biol. Crystallogr.* **67**, 303–312 (2011).
36. Ostermann, N., Gerhartz, B., Worpenberg, S., Trappe, J. & Eder, J. Crystal structure of an activation intermediate of cathepsin E. *J. Mol. Biol.* **342**, 889–899 (2004).
37. Emsley, P. & Cowtan, K. Coot: model-building tools for molecular graphics. *Acta Crystallogr. D Biol. Crystallogr.* **60**, 2126–2132 (2004).
38. Adams, P.D. *et al.* PHENIX: a comprehensive Python-based system for macromolecular structure solution. *Acta Crystallogr. D Biol. Crystallogr.* **66**, 213–221 (2010).